Two-Dimensional Short-Range Disordered Crystalline Networks from Flexible Molecular Modules

David Ecija,[†,*] Saranyan Vijayaraghavan,[†] Willi Auwärter,[†,*] Sushobhan Joshi,[†] Knud Seufert,[†] Claudia Aurisicchio,[‡] Davide Bonifazi,[§,*] and Johannes V. Barth[†]

[†]Physik Department E20, Technische Universität München, D-85748 Garching, Germany, [‡]Department of Chemistry, University of Namur, Rue de Bruxelles 61, B-5000, Namur, Belgium, and [§]Department of Pharmaceutical Sciences, University of Trieste, Piazzale Europa 1, I-34127, Trieste, Italy

ABSTRACT

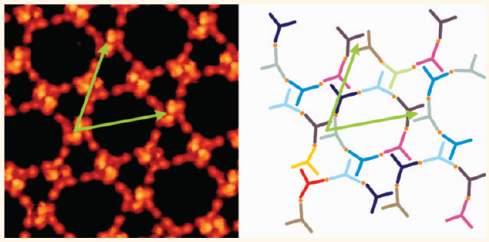

Studies of complex condensed matter systems have led to the discovery of materials of unexpected spatial organization as glasses, glassy crystals, quasicrystals, and protein and virus crystals. Here, we present *two-dimensional (2D) short-range disordered molecular crystalline networks*, which, regarding spatial organization, can be considered as surface analogues of 3D glassy crystals. In particular, the deposition of a flexible molecular module on Cu(111) gives rise to distinct phases whose characteristics have been examined in real space by scanning tunneling microscopy: a 2D short-range distortional disordered crystalline network and a 2D short-range orientational disordered crystalline network, respectively. Both phases exhibit a random arrangement of nanopores that are stabilized by the simultaneous presence of metal—organic and pyridyl—pyridyl interactions. The 2D short-range distortional disordered crystalline network displayed intriguing flexibility, as probed by the STM tip that modifies the pore shape, a prerequisite for adaptive behavior in host—guest processes.

KEYWORDS: 2D surface self-assembly · porous networks · supramolecular chemistry · STM

Unraveling the nature of complex condensed matter systems such as glasses, glassy crystals, quasicrystals, and protein and virus crystals is of paramount importance in actual materials science.[1−6] The traditional conception of a crystal based on translational symmetry has been widened upon the discovery of quasicrystals, and since 1992 a crystal is defined by the International Union of Crystallography as any solid having an essentially discrete diffraction pattern.[7] On the other hand, in three-dimensional (3D) materials science, an *amorphous solid* is considered as a material that possesses a noncrystalline structure.[8] In particular, it is called a *glass* if it undergoes a glass transition when heated to the liquid state.[2,8] In addition, a *molecular glassy crystal* is a material exhibiting a glass transition involving a rotational disorder of the constituting molecular units, whereas these constituents span a regular crystalline lattice.[9−17] Recently, by exploiting self-assembly protocols on surfaces,[18] two-dimensional (2D) supramolecular random networks have been fabricated on metallic surfaces and associated with glasses.[19,20] To simplify terminology (*cf.* Scheme 1b) and transferring the former definitions and concepts into the 2D space, in this paper we employ the term *2D short-range disordered crystalline network* to describe a 2D material that displays a discrete diffraction diagram and presents any of the following ordering characteristics: (1) the constituents are positioned following a crystalline lattice, but at the same time disordered with respect to their orientational or distortional degrees of freedom, or (2) the intermolecular links span a crystalline lattice, but the molecular building blocks present distortional (*cf.* bottom left of Scheme 1b) or orientational (*cf.* bottom right of Scheme 1b) short-range disorder. Therefore, regarding the spatial organization, a *2D short-range disordered crystalline network* may represent the surface analogue of a 3D glassy crystal, whereby a temperature dependent glass transition should be identified for certainty from the thermodynamic point of view.

Traditionally, most insights into the structure of noncrystalline materials have been based on diffraction techniques that rely on space averaging. Only recently the employment of self-assembly protocols on surfaces to create surface-confined supramolecular random networks and their *in situ*

* Address correspondence to david.ecija.fernandez@ph.tum.de; wilhelm.auwaerter@ph.tum.de; davide.bonifazi@fundp.ac.be.

Received for review February 22, 2012 and accepted April 4, 2012.

Published online April 04, 2012
10.1021/nn3007948

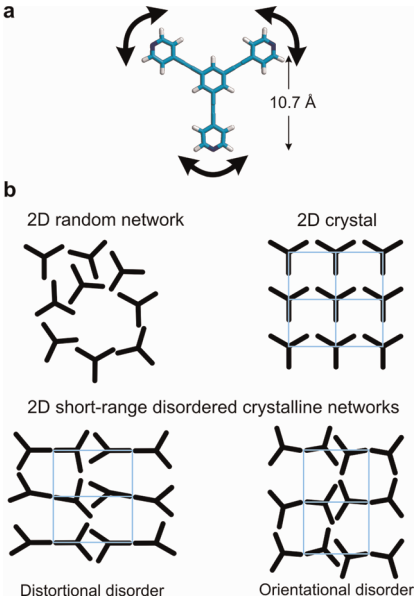

Scheme 1. (a) Schematic model of compound 1 (top view), in which molecular dimensions were obtained for an isolated molecule using the Hyperchem software (MM+ method). Black arrows indicate the flexibility of the terminal groups. (b) Types of assembly of a 2D supramolecular structure with different short- and long-range order characteristics for a tecton with 3-fold symmetry and geometrical flexibility. The blue network represents a crystalline lattice.

visualization with scanning tunneling microscopy (STM) provided crucial breakthroughs regarding the local order characteristics of the 2D amorphous structures.[19−22] The extension of this approach to other complex condensed matter systems could allow us to develop new materials and to greatly enhance our understanding of the physical phenomena associated with crystallization and vitrification, which are of crucial importance in a variety of fields such as pharmacology or materials science.

Regarding the supramolecular approach, for many surface-confined self-assembled nanostructures, the enthalpies associated with lateral intermolecular interactions are relatively weak, thus implying that a fine interplay of enthalpic and entropic contributions determines the final self-assembled pattern. In particular, upon formation of a nanostructure, freezing conformations of a flexible molecule can make loss of the conformational entropy more significant to the self-assembly process,[23] even leading to noncrystalline condensed matter states. The realization of 2D disordered systems thus requires a specific balance between molecule-surface and intermolecular interactions, and entropic contributions in the self-assembly to avoid the formation of patterns dictated by the surface lattice periodicity.

In this article, exploiting the self-assembly route to organize an inherently flexible molecular module (molecule **1**), we report the formation of 2D porous short-range disordered crystalline networks on Cu(111): a 2D short-range distortional disordered crystalline phase (α) and a 2D short-range orientational disordered crystalline phase (β). Our study visualizes with submolecular resolution a molecular self-assembly exhibiting simultaneously short-range disorder and crystalline long-range order. Furthermore, we probe the flexibility of the nanoporous phase α by inducing a flipping of the terminal groups with an STM tip, suggesting an adaptive behavior of the hosting networks toward molecular guests, a crucial property for exploitation in molecular recognition.[24,25] Consequently, phase α represents a "soft porous crystal" in 2D.[26]

RESULTS AND DISCUSSION

Molecule **1**, 1,3,5-tris(pyridin-4-ylethynyl)benzene, consists of three pyridyl groups connected to a central aryl ring through alkyne moieties (*cf.* Scheme 1a). The synthetic pathway employed for the preparation of **1** is reported in the Supporting Information. The functional terminal groups are programmed to steer metal−organic interactions through pyridyl−metal−pyridyl coordination motifs.[27−31] A key characteristic of this molecular module is the inherent flexibility of the substituents (≡CPyr) at the central aryl group, which can substantially deviate from the ideal 120° internal angle between two pyridin-4-ylethynyl peripheries, distorting the expected 3-fold symmetry. This phenomenon has been previously observed by us with porphyrin derivatives equipped with identical substituents exhibiting a distortional adaptation upon surface adsorption.[30,32]

The deposition of compound **1** on Cu(111), at a substrate temperature of 350 K, results in an assembly that exhibits polymorphism controlled by the coverage. Images taken at very low coverage (<0.01 ML) show that the molecular species completely decorate the steps before ordering on the terraces, indicating a high mobility at 350 K. For increased coverages below 0.2 ML, module **1** self-assembles in a 2D porous short-range distortional disordered crystalline network (phase α, *cf.* Figures 1a,c,d and 2). Phase α appears in coexistence with a minority 2D porous random network (*cf.* Figure 1a,b). At intermediate coverage (0.2−0.5 ML) phase α coexists again with residues of the 2D random network and an additional phase labeled β, which represents a 2D porous short-range orientational disordered crystalline network (*cf.* Figure SI 1 and Figure 3). At higher coverage (>0.5 ML), phase α is not detected and densely packed crystalline molecular islands emerge (phase γ, *cf.* Figure SI 2), coexisting with phase β domains, which diminish with the coverage. For all coverage ranges an annealing procedure close to the temperature of desorption ($T_{desorption} \approx 393$ K) had no noticeable impact on the organization. Whether the 2D short-range disordered crystalline phases are kinetically frustrated or thermodynamically stable is still under debate.

Low-Coverage Polymorphism. As depicted in Figure 1a, for coverages below 0.2 ML the deposition of compound

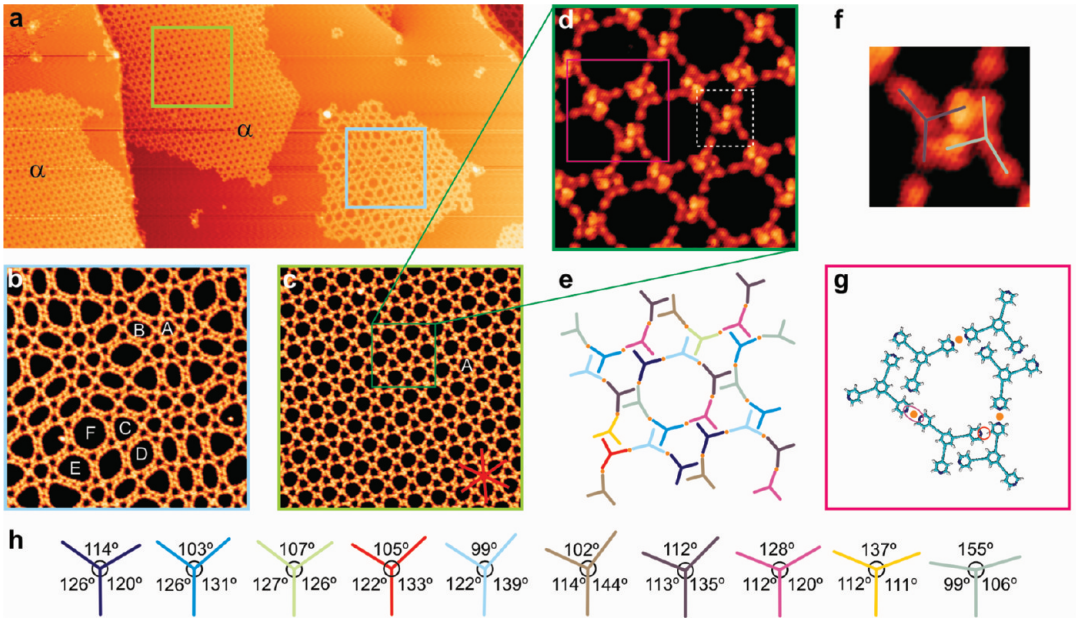

Figure 1. Self-assembly of compound 1 on Cu(111) into a 2D short-range distortional disordered crystalline network (phase α) coexisting with a 2D random network, for coverages below 0.2 ML. (a) Large-scale STM image displaying one 2D random network island (blue square) and two 2D short-range disordered crystalline islands (green square). (b) Zoom-in of the 2D random network region of part a. The different types of pores are labeled with the letters A, B, C, D, E, and F, respectively. (c) Zoom-in of the 2D short-range disordered crystalline region of part a. Only the pore of type A is present in this assembly. The red star represents the close-packed directions of Cu(111). (d) High-resolution STM image obtained with a CO-terminated tip depicted with submolecular resolution phase α. (e) Model of part d in the "stick" representation, in which each stick reflects the angular deviation from the ideal 3-fold molecular symmetry. Molecular units exhibiting the same apparent opening angles are depicted with the same colors. Cu adatoms are represented by an orange circle. (f) Zoom-in of the white-dotted area of part c and superposition of the stick model on two molecules. (g) Model of the two bonding motifs stabilizing the network: a 2-fold pyridyl−Cu−pyridyl bond (highlighted by a purple ellipse) and a pyridyl−pyridyl interaction (highlighted with a red circle). (h) Stick representation of the different molecular configurations of part d, called scissomers, as adapted upon surface adsorption. Image sizes: (a) 2963 × 1380 Å^2; (b, c) 443 × 443 Å^2; (d) 110 × 110 Å^2; (f) 25 × 25 Å^2. Tunneling parameters: (a−c) I = 0.03 nA, V_b = 1 V; (d, f) I = 0.05 nA, V_b = −0.075 V.

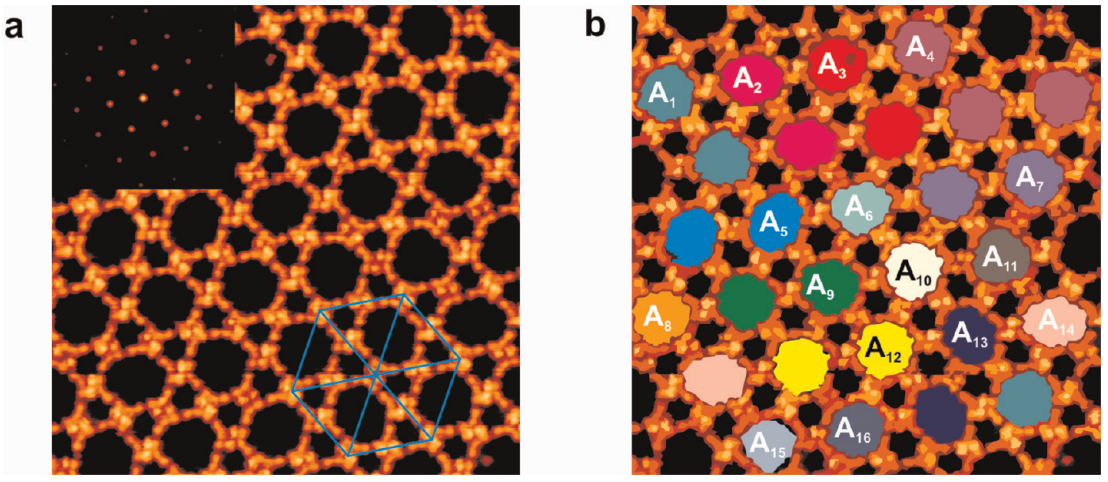

Figure 2. Self-assembly of compound 1 into a molecular 2D short-range distortional disordered crystalline network (phase α). High-resolution STM images of an arrangement of type A pores in phase α. (a) The inset displays the autocorrelation plot of the figure. Blue lines are used to describe the repeating motif with a unit cell vector length of 44 Å. (b) Filling of the pores by assigning one color to each type of pore. The different pores are labeled with the term A_n (from A_1 to A_{16}). Image sizes: (a, b) 242 × 242 Å^2. Tunneling parameters: (a, b) I = 0.052 nA, V_b = −0.075 V.

1 results in the formation of a 2D porous short-range distortional disordered crystalline network (phase α, *cf.* Figure 1c) that coexists with a minority 2D porous random network (*cf.* Figure 1b). For clarity, the structural nature of phase α as a 2D short-range disordered crystalline network will be addressed below. Phase α is based on pores formed by the combination of six molecules (named as pores A), whereas the 2D random network exhibits pores formed by six, eight, nine, 10, 11, and 12 molecules (named as pores A, B, C, D, E, and F,

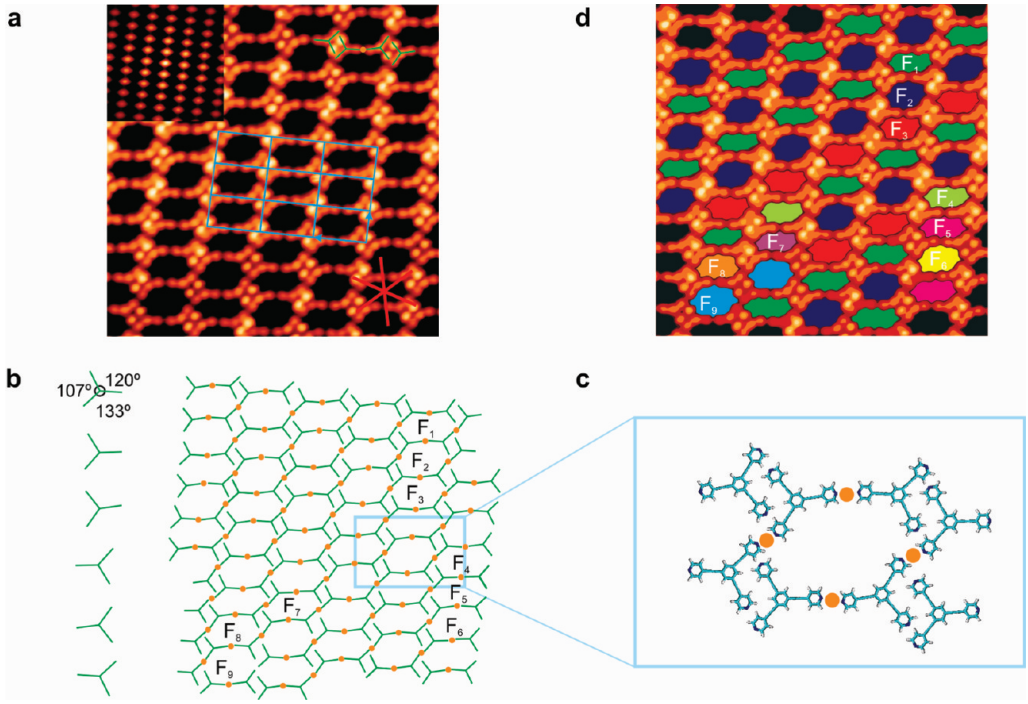

Figure 3. Self-assembly of compound 1 into a supramolecular 2D short-range orientational disordered crystalline network. (a) High-resolution STM image depicting different types of rectangular pores. To clarify the appearance of the molecular units, a green "stick" molecular model is superimposed on the top right of the image. The inset represents the autocorrelation plot of the image. The repeating motif is displayed as a blue lattice with unit cell vector lengths of 29.5 and 17.7 Å. The red star represents the close-packed directions of Cu(111). (b) Model of part a in the "stick" representation, in which each stick reflects the angular deviation from the in-gas 3-fold molecular symmetry. Molecular units exhibit the same configuration (scissomer) and six different orientations upon adsorption on the surface. (c) Model of the two bonding motifs stabilizing the network: a 2-fold pyridyl−Cu−pyridyl bond and a lateral pyridyl−pyridyl interaction. In a−c Cu adatoms are represented by orange circles. (d) Filling of the pores of part a, assigning one color to each type of pore and labeling them with the term F_n (from F_1 to F_9). Images size (a, d): 184 × 184 Å^2. Tunneling parameters: I = 0.2 nA, V_b = −0.2 V.

respectively, *cf*. Figure 1b and Figure SI 3). Remarkably, phase α and the 2D random network share pore A as a constituent motif. A statistical analysis of the fractional pore occurrence at ∼0.2 ML coverage reveals a distribution where pores of type A dominate (∼60%), followed by those of type B (∼20%). With a probability of less than 10%, bigger pores of type C (∼9%), D (∼9%), and F (∼2%) are observed. Rarely, pores constituted of 11 molecules were also detected (named as pore E, *cf*. Figure 1b).

High-resolution data (*cf*. Figure 1d,f) allow us to discern individual molecules with submolecular features. Each molecule is characterized by four lobes, which correspond to the central aryl and the three peripheral pyridyl groups, respectively. Importantly, the molecular appearance in the STM images deviates from a strict 3-fold symmetry (*cf*. Scheme 1), which highlights the intrinsic flexibility of molecule **1** upon adsorption on Cu(111). Herein, a minor contribution of the out-of-plane rotation of the pyridyl terminal groups cannot be neglected.[33] A structural analysis reveals apparent opening angles between pyridin-4-ylethynyl functions ranging from 99° to 155° (cf. Figure 1e and h). The intramolecular flexibility is the major element for the formation of the 2D short-range disordered crystalline networks and the minority 2D random network, respectively, as it leads to multiple configurations of the molecule,[34] designated *scissomers*, in analogy with the scissoring vibrational mode. In addition, as clearly displayed in Figure 1d, the networks exhibit two different recognition motifs (*cf*. Figure 1g): (i) a head-to-head orientation between two "dim" pyridyl groups of neighboring molecules with a projected N−N distance of 3.4 ± 0.4 Å[27−31] and (ii) an interaction of one bright pyridyl group per molecule with an adjacent pyridyl ring. The latter motif is assigned to a noncovalent interaction with a characteristic N−H length of 1.8 ± 0.4 Å, similarly identified at the liquid−solid interface.[35] The pyridyl groups involved in this lateral pyridyl−pyridyl interaction are visualized as bright protrusions independent of the applied bias voltage, suggesting a nonparallel orientation of the heteroaromatic ring relative to the surface. Based on the N−N spacing and previous reports, motif (i) is identified as a pyridyl−Cu−pyridyl metal−organic interactions, where the mediating Cu adatom (supplied by the surface)[36,37] is not resolved.[27,29,30,38−40] Summarizing, each molecule is engaged in two metal−organic coordination bonds and two lateral pyridyl−pyridyl contacts. This demonstrates for the first time a simultaneous

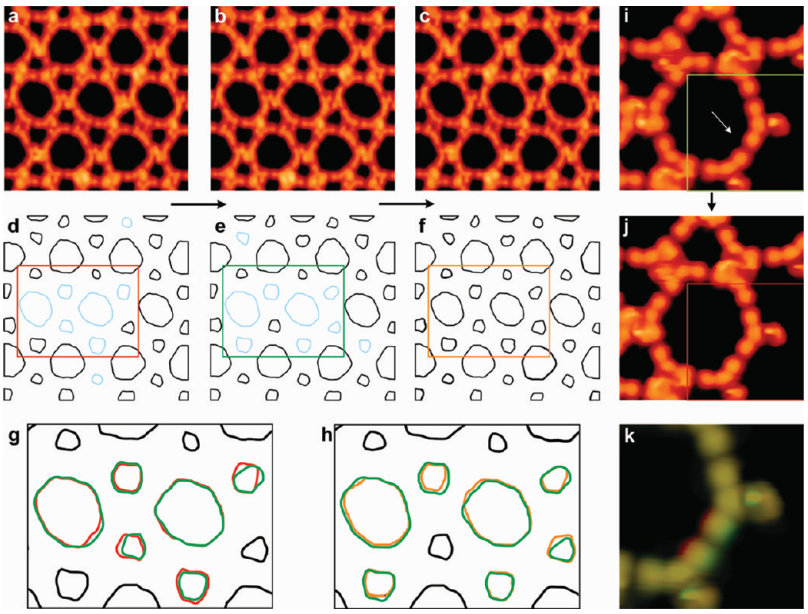

Figure 4. Dynamics of the α-short-range disordered crystalline network induced and probed by scanning with an STM tip. STM images of an (a) initial, (b) intermediate, and (c) final configuration of an assembly of phase α, after recording three subsequent STM images. (d–f) Vectorization of images a–c, respectively, outlining the contour of the pores by a trace. Blue line in d and e represents those pores that change their shape while scanning from d to e and from e to f, respectively. (g) Zoom-in and superposition of parts d (red rectangle) and e (green rectangle). (h) Zoom-in and superposition of parts e and f (orange rectangle). Black line is used to depict those pores that do not modify their shape, whereas red, green, and orange lines represent pores of d, e, and f, respectively, which change their shape while scanning from one image to another. (i, j) Initial and final configuration of a pore of type A at the border of an assembly, displaying the change in geometry of the pyridyl–Cu–pyridyl bond, marked with a white arrow. (k) Superposition of a zoom-in of images i (green rectangle) and j (red rectangle), to address the change between both images. Images sizes: (a–c) 140 × 140 Å^2; (i, j) 48 × 48 Å^2, (k) 29 × 29 Å^2. Tunneling parameters: (a–c) I = 0.1 nA, V_b = −0.7 V; (i, k) I = 0.1 nA, V_b = −0.07 V.

expression of these two different interactions, in contrast to previous studies based on the same terminal functional groups, where only a metal–organic interaction dominates.[27,29−31] The prevalent expression of type A pores signals a more favorable bonding configuration as compared to pores of types B and C.[41]

2D Short-Range Distortional Disordered Crystalline Network. A close inspection of phase α reveals it to be constituted by pores of type A with slightly different shapes and a mean area of 576 Å^2, which combine in an assembly exhibiting long-range order (*cf.* Figure 2). The corresponding 2D autocorrelation plot, a mathematical technique to identify repeating patterns by depicting the cross-correlation of a measured image with itself, clearly shows a 6-fold symmetric pattern with a periodicity of 44 Å (*cf.* inset of Figure 2a), with a deviation of 1.5 ± 0.5 Å, deriving from identical oriented protruding pyridyl–pyridyl contacts. These results are in full agreement with the fast Fourier transformation of the same image (not displayed). Due to the flexibility of the pyridin-4-ylethynyl legs, the molecules present distortions through the assembly, giving rise to pores A of different shapes (labeled with subscripts A_n in Figure 2b), which are responsible for the deviation of the lateral pyridyl–pyridyl motifs from a perfect lattice. Herein, the influence of the substrate is manifested in the presence of two organizational chiral domains, in which the lattice of the pyridyl–pyridyl contacts is rotated 25° ± 5° in chirality of type I and −25° ± 5° in chirality of type II with respect to the close-packed directions of Cu(111) (*cf.* Figure 1c, 1d and 2a for chirality of type I). On the basis of the features of a 2D short-range disordered crystalline network introduced in the first paragraph and considering the deviation due to the flexibility of the modules, we conclude that phase α represents a molecular 2D short-range distortional disordered crystalline network. This visualization of a supramolecular 2D short-range disordered crystalline network represents a distinct condensed-matter state as compared to well-established 2D crystalline phases or 2D random networks. To our knowledge, these types of molecular architectures exhibiting a coexistence of amorphous and highly correlated structural features have been observed at the 3D mesoscale, for example in virus crystals,[42] with a potential 2D analogue reported for a dense-packed assembly at the nanoscale,[43] though not recognized as such.

2D Short-Range Orientational Disordered Crystalline Network. For coverages exceeding 0.2 ML a second 2D short-range disordered crystalline phase appears. Figure 3a depicts a high-resolution image of the molecular assembly in phase β, in which, as in phase α, the molecular appearance deviates from a 3-fold symmetry. However, in contrast to phase α and with-

in the limits of the STM intramolecular resolution, we identify only a single molecular configuration (scissomer) constituting phase β, which exhibits apparent intramolecular opening angles between two pyridin-4-ylethynyl peripheries of 107°, 120°, and 133°, respectively. In addition, we distinguish six different molecular orientations of the scissomer (*cf.* Figure 3b). The bonding motifs of the assembly are identical to phase α; that is, each molecule presents two lateral pyridyl−pyridyl contacts and two pyridyl−Cu−pyridyl links with adjacent molecules (*cf.* Figure 3c). However, the density and topology of phase β differ from phase α: in phase β the links between adjacent pores rely on pyridyl−Cu−pyridyl bonds, whereas in phase α the connection between pores is solely based on the lateral pyridyl−pyridyl interactions. The resulting porous network comprises different pores of rhombic shape, with a mean area of 184 Å^2, each one characterized by a particular combination of orientations of the scissomers. The repeatedly observed pore shapes are labeled in Figure 3b,d (F_1 to F_9) and displayed with a color-coded filling in Figure 3d. Within the assembly, the spatial distribution of the pore shapes is random (Figure 3d). Nevertheless, the autocorrelation plot of the assembly (inset of Figure 3a) displays a periodic order with a rectangular repeating motif of size 29.5 Å × 17.7 Å, defined by the lateral pyridyl−pyridyl contacts (see blue rectangular lattice in Figure 3a). Herein, the influence of the substrate is again visualized by the presence of a chiral organization, constituted by three orientational domains per chirality, giving a total of six domains, in which the long unit vector of the lattice of the lateral pyridyl−pyridyl contacts forms an angle of 17° ± 5° in chirality of type I and −17° ± 5° in chirality of type II with respect to the close-packed directions of Cu(111) (*cf.* Figure 3a for chirality of type I). Thus, by analogous arguments to those used for the description of phase α, we conclude that the assembly of phase β constitutes a 2D short-range orientational disordered crystalline network.

The origin of these 2D short-range disordered crystalline networks is tentatively attributed to substrate-mediated effects, since the deposition of the very same building block on Ag(111) exclusively yields regular crystalline networks, exhibiting both short- and long-range order. On the other hand, the emergence of phase β at increased coverage together with the nucleation of phase β within α islands hints toward in-plane compression[44] as a plausible driving mechanism for this transition.

The molecular flexibility resulting in different configurations upon adsorption that deviate from a strict 3-fold symmetry is a key ingredient for the assembly of the above-discussed 2D short-range disordered crystalline network and of interest for engineering functional templating structures. Remarkably, the flexibility of the pyridin-4-ylethynyl substituents at the central aryl group is directly proven by STM experiments that can simultaneously induce and visualize distorsional changes in the networks. To this aim, we altered the STM scanning conditions that were initially established to image the assembly under nonperturbative conditions. Thus, it was possible to induce modifications of the networks and directly observe the resulting temporal variations of the pore shapes in phase α (*cf.* Figure 4a−h and movie in the Supporting Information). A detailed analysis reveals that these alterations are mediated by a subtle variation in the opening angle of the pyridin-4-ylethynyl legs involved in the 2-fold pyridyl−Cu−pyridyl bond, thus inducing a change in the size and shape of some pores (*cf.* Figure 4i−k). This intrinsic flexibility of the metal−organic motif has been already observed for porphyrin-based coordination polymers on Cu(111) presenting the same substituents.[29,32] It was attributed to the inherent flexibility of the substituted leg (≡CPyr, *cf.* Figure SI 4) combined with a low-energy cost for deflecting the pyridyl−Cu−pyridyl bond angle away from 180°.

Our results suggest that phase α represents a soft porous crystal in 2D. Analogous materials are established in 3D as third-generation porous coordination polymers, bearing significant promise in the field of host−guest complexation, because they exhibit dynamic frameworks that are able to respond/adapt to external stimuli such as light, electric fields, or particular guest species, while retaining high mesoscale regularity.[26]

CONCLUSIONS

In summary, we reported experimental evidence for supramolecular 2D short-range disordered crystalline networks. These structures are potential 2D analogues to established 3D molecular glassy crystals. They have been produced on a Cu(111) support by exploiting supramolecular self-assembly protocols relying on a programmed flexible molecular module and characterized at the molecular level by scanning tunneling microscopy. These 2D short-range disordered crystalline networks are stabilized by a combination of lateral pyridyl−pyridyl links and metal−organic bonds. The intermolecular pyridyl−pyridyl links follow a regular lattice, but through the network either the distortion (phase α) or the orientation of the molecular modules (phase β) is random. Two coexisting 2D short-range disordered crystalline networks exhibiting a different topology were observed at intermediate molecular coverage. One is described by a rectangular repeating motif in the autocorrelation plot (phase β), whereas the other one exhibits a hexagonal symmetry (phase α). The flexibility of phase α is addressed via STM stimuli, which results in slight distorsional changes of the pores, whereby the network structure is retained. This behavior implies a 2D representation of soft porous crystals, suggesting a dynamic adaptive behavior, crucial in molecular recognition and self-repairing processes. In this sense, the simultaneous stabilization by metal−organic coordination bonds and pyridyl−pyridyl links provides an advantageous balance between robustness and adaptability for future applications. Altogether,

our results underline the potential of 2D-metallosupramolecular chemistry[45,46] to open new avenues toward the fabrication and understanding of novel nanostructured condensed matter systems.

METHODS

All STM experiments were performed in a custom-designed ultrahigh-vacuum system providing a base pressure below 1×10^{-10} mbar.[47] The monocrystalline Cu(111) substrate was cleaned by repeated Ar^+ sputtering cycles at an energy of 800 eV, followed by annealing at 730 K for 10 min. Subsequently, a submonolayer coverage of molecular derivative **1** was deposited by organic molecular beam epitaxy from a thoroughly degassed quartz crucible held at 463 K. During deposition of module **1** the Cu(111) surface was kept at 343 K and the pressure remained at $<5 \times 10^{-10}$ mbar. All data were acquired employing a low-temperature CreaTec-STM[48] with the sample held at 6 K using electrochemically etched W tips. In the figure captions, V_b refers to the bias voltage applied to the sample. Simulations were performed in the framework of the Hyperchem 7.5 software package.[49]

Conflict of Interest: The authors declare no competing financial interest.

Acknowledgment. We thank Dr. Joachim Reichert, Dr. Emmanuel Arras, Dr. Carlos-Andrés Palma, and Dr. Francesco Allegretti for fruitful discussions. Work was supported by the ERC Advanced Grant MolArt (no. 247299), the German Research Foundation (DFG) through BA 3395/2-1, the TUM-IAS, and the Munich Center for Advanced Photonics (MAP). D.E. thanks the European Commission for support through the Marie Curie IntraEuropean Fellowship for Career Development FP7 program (project Nanolanta, no. 235722). D.B. thanks the FRS-FNRS (FRFC contract nos. 2.4.550.09 and 2.4.617.07.F and MIS no. F.4.505.10. F), the "Loterie Nationale", the "TINTIN" ARC project (contract no. 09/14-023), the Région Wallonne through the "SOLWATT" program (SUNTUBE, no. 850551), and the University of Namur (internal funding).

Supporting Information Available: Synthetic scheme and procedure of molecule **1**. STM image of the coexistence of phases α and β at intermediate coverage (0.2−0.5 ML). High-resolution STM image of the crystalline network formed by compound **1** on Cu(111) at coverages above 0.5 ML. High-resolution STM images of the different pores that form the α-phase. Movie showing the shape variations of pores within an α-phase island during scanning with an STM tip. High-resolution STM images depicting the flexibility of module **1**. This material is available free of charge *via* the Internet at http://pubs.acs.org.

REFERENCES AND NOTES

1. Angell, C. A. Formation of Glasses from Liquids and Biopolymers. *Science* **1995**, *267*, 1924–1935.
2. Debenedetti, P. G.; Stillinger, F. H. Supercooled Liquids and the Glass Transition. *Nature* **2001**, *410*, 259–267.
3. Chandler, D. Liquids: Condensed, Disordered, and Sometimes Complex. *Proc. Natl. Acad. Sci. U. S. A.* **2009**, *106*, 15111–15112.
4. Shechtman, D.; Blech, I.; Gratias, D.; Cahn, J. W. Metallic Phase with Long-Range Orientational Order and No Translational Symmetry. *Phys. Rev. Lett.* **1984**, *53*, 1951–1954.
5. Ilari, A.; Savino, C. Protein Structure Determination by X-ray Crystallography. *Methods Mol. Biol.* **2008**, *452*, 63–87.
6. Fry, E. E.; Grimes, J.; Stuart, D. I. Virus Crystallography. *Mol. Biotechnol.* **1999**, *12*, 13–23.
7. Steurer, W.; Deloudi, S. Fascinating Quasicrystals. *Acta Crystallogr.* **2007**, *A64*, 1–11.
8. Zallen, R. *The Physics of Amorphous Solids*; Wiley: New York, 2004.
9. Adachi, K.; Suga, H.; Seki, S. Phase Changes in Crystalline and Glassy-Crystalline Cyclohexanol. *Bull. Chem. Soc. Jpn.* **1968**, *41*, 1073–1087.
10. Foulon, M.; Amoureux, J. P.; Sauvajol, J. L.; Lefebvre, J.; Descamps, M. Evidence of a 'Glassy Crystal' Phase Obtained by the Quenching of the Plastic Phase of the Cyanoadamantane. *J. Phys. C: Solid State Phys.* **1983**, *16*, L265–L269.
11. Pathmanathan, K.; Johari, G. P. Molecular Relaxations in a Rigid Molecular Glassy Crystal. *J. Phys. C: Solid State Phys.* **1985**, *18*, 6535–6545.
12. Lefebvre, J.; Rolland, J. P.; Sauvajol, J. L.; Hennion, B. Coherent Neutron Scattering on the 'Glassy Crystal' of Cyanoadamantane. *J. Phys. C: Solid State Phys.* **1985**, *18*, 241–255.
13. Descamps, M.; Willart, J. F.; Delcourt, O. Molecular and Structural Relaxations in a Glassy Crystal. *Phys. A* **1993**, *201*, 346–362.
14. Willart, J. F.; Descamps, M.; Benzakour, N. Polymorphism of a Glass Forming Plastic Crystal: A Kinetic Investigation *J. Chem. Phys.* **1996**, *104*, 2508–2517.
15. Delcourt, O.; Descamps, M.; Even, J.; Bertault, M.; Willart, J. F. Peculiarities of the Enthalpy Relaxation of a Glassy Crystal. *Chem. Phys.* **1997**, *215*, 51–57.
16. Kuchta, B.; Descamps, M.; Affouard, F. A Monte Carlo Study of Metastable Structures of the Cyanoadamantane Crystal. *J. Chem. Phys.* **1998**, *109*, 6753–6763.
17. Brand, R.; Lunkenheimer, P.; Loidl, A. Relaxation Dynamics in Plastic Crystals. *J. Chem. Phys.* **2002**, *116*, 10386–10401.
18. Barth, J. V. Molecular Architectonic on Metal Surfaces. *Annu. Rev. Phys. Chem.* **2007**, *58*, 375–407.
19. Otero, R.; Lukas, M.; Kelly, R. E. A.; Xu, W.; Lagsgaard, E.; Stensgaard, I.; Kantorovich, L. N.; Besenbacher, F. Elementary Structural Motifs in a Random Network of Cytosine Adsorbed on a Gold(111). *Surf. Sci.* **2008**, *319*, 312–315.
20. Marschall, M.; Reichert, J.; Weber-Bargioni, A.; Seufert, K.; Auwärter, W.; Klyatskaya, S.; Zoppellaro, G.; Ruben, M.; Barth, J. V. Random Two-Dimensional String Networks Based on Divergent Coordination Assembly. *Nat. Chem.* **2010**, *2*, 131–137.
21. Blunt, M. O.; Russell, J. C.; Giménez-López, M. d. C.; Garrahan, J. P.; Lin, X.; Schröder, M.; Champness, N. R.; Beton, P. H. Random Tiling and Topological Defects in a Two-Dimensional Molecular Network. *Science* **2008**, *322*, 1077–1081.
22. Pivetta, M.; Blüm, M.-C.; Patthey, F.; Schneider, W.-D. Two-Dimensional Tiling by Rubrene Molecules Self-Assembled in Supramolecular Pentagons, Hexagons, and Heptagons on a Au(111) Surface. *Angew. Chem., Int. Ed.* **2008**, *47*, 1076–1079.
23. Whitesides, G. M.; Mathias, J. P.; Seto, C. T. Molecular Self-Assembly and Nanochemistry: A Chemical Strategy for the Synthesis of Nanostructures. *Science* **1991**, *254*, 1312–1319.
24. Kriwacki, R. W.; Hengst, L.; Tennant, L.; Reed, S. I.; Wright, P. E. Structural Studies of $p21^{Waf1/Cip1/Sdi1}$ in the Free and Cdk2-Bound State: Conformational Disorder Mediates Binding Diversity. *Proc. Natl. Acad. Sci. U. S. A.* **1996**, *93*, 11504–11509.
25. Mittag, T.; Kay, L. E.; Forman-Kay, J. D. Protein Dynamics and Conformatinal Disorder in Molecular Recognition. *J. Mol. Recognit.* **2010**, *23*, 105–116.
26. Horike, S.; Shimomura, S.; Kitagawa, S. Soft Porous Crystals. *Nat. Chem.* **2009**, *1*, 695–704.
27. Tait, S. L.; Langner, A.; Lin, N.; Stepanow, S.; Rajadurai, C.; Ruben, M.; Kern, K. One-Dimensional Self-Assembled Molecular Chains on Cu(100): Interplay Between Surface-Assisted Coordination Chemistry and Substrate Commensurability. *J. Phys. Chem. C* **2007**, *111*, 10982–10987.
28. Eichberger, M.; Marschall, M.; Reichert, J.; Weber-Bargioni, A.; Auwärter, W.; Wang, R. L. C.; Kreuzer, H. J.; Pennec, Y.; Schiffrin, A.; Barth, J. V. Dimerization Boosts One-Dimensional Mobility

of Conformationally Adapted Porphyrins on a Hexagonal Surface Atomic Lattice. *Nano Lett.* **2008**, *8*, 4608–4613.
29. Heim, D.; Seufert, K.; Auwärter, W.; Aurisicchio, C.; Fabbro, C.; Bonifazi, D.; Barth, J. V. Surface-Assisted Assembly of Discrete Porphyrin-Based Cyclic Supramolecules. *Nano Lett.* **2009**, *10*, 122–128.
30. Heim, D.; Ecija, D.; Seufert, K.; Auwärter, W.; Aurisicchio, C.; Fabbro, C.; Bonifazi, D.; Barth, J. V. Self-Assembly of Flexible One-Dimensional Coordination Polymers on Metal Surfaces. *J. Am. Chem. Soc.* **2010**, *132*, 6783–6790.
31. Shi, Z.; Liu, J.; Lin, T.; Xia, F.; Liu, P. N.; Lin, N. Thermodynamics and Selectivity of Two-Dimensional Metallo-Supramolecular Self-Assembly Resolved at Molecular Scale. *J. Am. Chem. Soc.* **2011**, *133*, 6150–6153.
32. Écija, D.; Seufert, K.; Heim, D.; Auwärter, W.; Aurisicchio, C.; Fabbro, C.; Bonifazi, D.; Barth, J. V. Hierarchic Self-Assembly of Nanoporous Chiral Networks with Conformationally Flexible Porphyrins. *ACS Nano* **2010**, *4*, 4936–4942.
33. Piot, L.; Silly, F.; Tortech, L.; Nicolas, Y.; Blanchard, P.; Roncali, J.; Fichou, D. Long-Range Alignments of Single Fullerenes by Site-Selective Inclusion into a Double-Cavity 2D Open Network. *J. Am. Chem. Soc.* **2009**, *131*, 12864–12865.
34. According to Eliel, E. L.; Wilen, S. H. In *Stereochemistry of Organic Compounds*; 1994; pp 19−20, "the most fundamental distinction one can make between configuration and conformation, is to say that configurational differences imply differences in bond angles, whereas conformational differences involve differences in torsion angles (including in both case, differences, that are exclusively in sign)." On the basis of this distinction, molecules of identical constitution but differing in bond angles (*cf.* Figure 1h) can be thus considered configurational isomers.
35. Zhang, X.; Chen, T.; Yan, H.-J.; Wang, D.; Fan, Q.-H.; Wan, L.-J.; Ghosh, K.; Yang, H.-B.; Stang, P. J. Engineering of Linear Molecular Nanostructures by a Hydrogen-Bond-Mediated Modular and Flexible Host-Guest Assembly. *ACS Nano* **2010**, *4*, 5685–5692.
36. Perry, C. C.; Haq, S.; Frederick, B. G.; Richardson, N. V. Face Specificity and the Role of Metal Adatoms in Molecular Reorientation at Surfaces. *Surf. Sci.* **1998**, *409*, 512–520.
37. Lin, N.; Dmitriev, A.; Weckesser, J.; Barth, J. V.; Kern, K. Real-Time Single-Molecule Imaging of the Formation and Dynamics of Coordination Compounds. *Angew. Chem., Int. Ed.* **2002**, *41*, 4779–4783.
38. Classen, T.; Fratesi, G.; Costantini, G.; Fabris, S.; Stadler, F. L.; Kim, C.; Gironcoli, S. d.; Baroni, S.; Kern, K. Templated Growth of Metal−Organic Coordination Chains at Surfaces. *Angew. Chem., Int. Ed.* **2005**, *44*, 6142–6145.
39. Schlickum, U.; *et al.* Metal-Organic Honeycomb Nanomeshes with Tunable Cavity Size. *Nano Lett.* **2007**, *7*, 3813–3817.
40. Klappenberger, F.; Weber-Bargioni, A.; Auwärter, W.; Marschall, M.; Schiffrin, A.; Barth, J. V. Temperature Dependence of Conformation, Chemical State, and Metal-Directed Assembly of Tetrapyridyl-Porphyrin on Cu(111). *J. Chem. Phys.* **2008**, *129*, 214702.
41. Palma, C.-A.; Bjork, J.; Bonini, M.; Dyer, M. S.; Llanes-Pallas, A.; Bonifazi, D.; Persson, M.; Samorì, P. Tailoring Bicomponent Supramolecular Nanoporous Networks: Phase Segregation, Polymorphism, and Glasses at the Solid-Liquid Interface. *J. Am. Chem. Soc.* **2009**, *131*, 13062–13071.
42. *Nanoscale Structure and Assembly at Solid Fluid Interfaces*; Kluwer Academic Publishers: New York, 2004; Vol. II.
43. Soubatch, S.; Temirov, R.; Tautz, F. S. Molecular Flexibility as a Factor Affecting the Surface Ordering of Organic Adsorbates on Metal Substrates. *Langmuir* **2006**, *22*, 9572–9579.
44. Liu, J.; Lin, T.; Shi, Z.; Xia, F.; Dong, L.; Liu, P. N.; Lin, N. Structural Transformation of Two-Dimensional Metal-Organic Coordination Networks Driven by Intrinsic In-Plane Compression. *J. Am. Chem. Soc.* **2011**, *133*, 18760–18766.
45. Lin, N.; Stepanow, S.; Ruben, M.; Barth, J. V. Surface-confined Supramolecular Coordination Chemistry. *Top. Curr. Chem.* **2009**, *287*, 1–44.
46. Barth, J. V. Fresh Perspectives for Surface Coordination Chemistry. *Surf. Sci.* **2009**, *603*, 1533–1541.
47. Auwärter, W.; Schiffrin, A.; Weber-Bargioni, A.; Pennec, Y.; Riemann, A.; Barth, J. V. Molecular Nanoscience and Engineering on Surfaces. *Int. J. Nanotechnol.* **2008**, *5*, 1171–1193.
48. Createc, D-74391 Erligheim, Germany.
49. *Hyperchem*, 32601, Gainesville, FL, USA.